JOURNAL OF COMPUTATIONAL PHYSICS 11, 210–239 (1973)

Accuracy Studies of the Numerical Method of Characteristics for Axisymmetric, Steady Supersonic Flows

JOE D. HOFFMAN

Associate Professor of Mechanical Engineering, Purdue University, Lafayette, Indiana 47907

Received August 26, 1971

A detailed numerical study of the accuracy of the method of characteristics is presented for axisymmetric, supersonic flows. Ten numerical schemes and three grid networks were investigated for both irrotational and rotational flows. In all cases, the Euler predictor–corrector difference scheme was employed, and studies were conducted with predict only, predict–correct, and repetitive application of the corrector. The results illustrate the general character of the various schemes, and some general observations are drawn.

1. INTRODUCTION

A survey of the method of characteristics for nonequilibrium, internal flows was presented by Sedney [1]. Several numerical schemes were reviewed, and some general conclusions were drawn. However, it is obvious from this survey that there is very little quantitative information available concerned specifically with establishing the accuracy of the various numerical schemes. The present paper presents some typical results of a numerical study of the accuracy of the method of characteristics for axisymmetric, supersonic steady flows. The limited study conducted by Giese [2] is the only such study found in the open literature.

In irrotational flow, two characteristic curves exist: right- and left-running Mach lines. In rotational flows, an additional characteristic curve exists—the streamline. Various grid schemes can be devised based on these characteristic curves, several of which are illustrated in Fig. 1. The inverse schemes illustrated in Figs. 1a and 1b consist of specifying points in a solution surface at which the properties are desired, and then constructing a grid by running characteristics back until they intersect the previous solution plane. Initial values are then found by interpolation. The direct schemes illustrated in Figs. 1c–f consist of running characteristics forward from known initial points until they intersect. For irrotational flow where only two families of characteristics exist, the unique grid scheme illustrated in Fig. 1c is determined. However, for rotational flows where three families of characteristics exist, three choices of grid scheme exist depending on which two of the

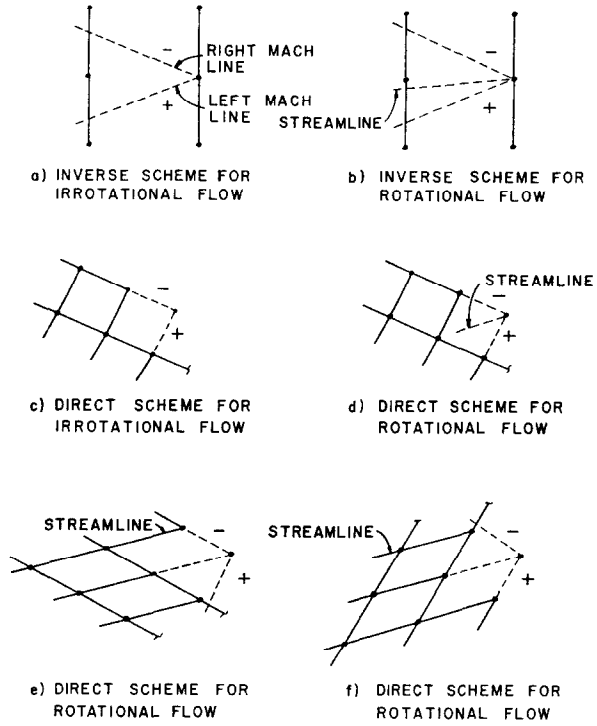

FIG. 1. General description of possible characteristic grid schemes.

three characteristics are chosen to define the solution point. These choices are illustrated in Figs. 1d-f. As discussed by Sedney, for dissipative flows such as nonequilibrium, reacting flows or gas-particle flows, grid schemes following the streamline and either Mach line are preferred for reasons of stability and accuracy. However, for nondissipative, rotational flows, there is no apparent reason why one scheme should be preferred over the others. The present paper is concerned with irrotational and nondissipative rotational flows based on the grid schemes illustrated in Figs. 1c and 1d, both of which are based on following distinct families of right- and left-running Mach lines.

For the rotational flow scheme, a degree of freedom still exists in the selection of the initial point on the rearward running streamline. Three possibilities are illustrated in Fig. 2. Grid scheme I continues the rearward running streamline back into the known data region until it intersects the first right-running Mach line in its path. Another scheme not shown, could be based on intersecting the first left Mach line. Grid scheme II extends the streamline back until it intersects either the first right Mach line or left Mach line in its path. Grid scheme III

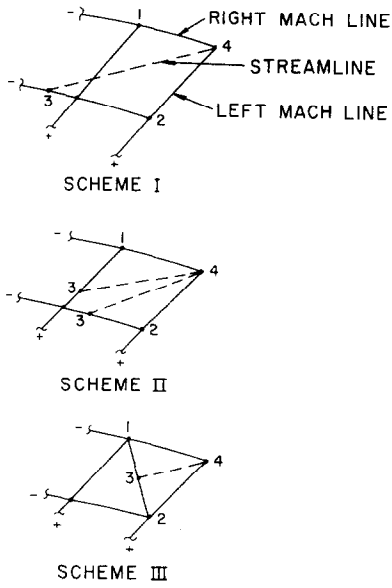

FIG. 2. Characteristic grid schemes I, II, and III for rotational flows.

extends the streamline back until it intersects the diagonal drawn between points 1 and 2. Once the back point has been determined by one of these three methods, a choice of interpolation schemes must be made for determining the flow properties at the back point. All three grid schemes were investigated in the present study. In grid scheme I, a cubic interpolating polynomial was employed along the right Mach line. In grid schemes II and III, linear interpolation was used. It was found that all three schemes resulted in comparable accuracy, so the bulk of the numerical work presented herein was conducted with grid scheme III, which is a more direct extension of the irrotational flow grid scheme.

Once the choice of grid scheme and interpolation technique have been made, the form of the compatibility equations valid on each characteristic must be determined, and the finite difference scheme employed for solving the compatibility equations must be chosen. Here again, many choices are available, all theoretically equivalent. The various forms which the compatibility equations can assume are developed in the next section. All are investigated numerically in the present study. The finite difference scheme generally, if not always, employed in the numerical method of characteristics is the modified Euler predictor–corrector scheme. Even in this scheme several choices exist for the evaluation of the coefficients in the compatibility equations. For example, the coefficients could be evaluated based on the average values of the properties along each characteristic, or they could be evaluated as average values of the coefficients along each char-

acteristic. Both schemes are theoretically second order, and both were investigated numerically to determine which, if either, was more accurate.

Thus, a bewildering choice of numerical schemes are available for the analysis of axisymmetric, steady supersonic flow by the numerical method of characteristics. The present paper presents the results of an extensive numerical investigation of a large number of these schemes in an attempt to determine the better approaches. Obviously, the results are only valid exactly for the flows considered. However, it is felt that many of the trends found are general in nature. It is hoped that other investigators may conduct similar investigations for other flows and other finite differences schemes, and eventually a much better understanding of the accuracy of the numerical method of characteristics will evolve.

II. Analysis

Since the theoretical development of the method of characteristics for axisymmetric, supersonic steady flow is well known, only the results needed here to develop the finite difference schemes will be considered. For irrotational flow, the governing equations are the gas dynamic equation and the irrotationality condition:

$$(u^2 - a^2)\, u_x + (v^2 - a^2)\, v_y + 2uvu_y - \delta a^2 v/y = 0, \tag{1}$$

$$u_y - v_x = 0. \tag{2}$$

For irrotational flow, the speed of sound a is a known function of the velocity. In Eq. (1), $\delta = 1$ for axisymmetric flow and 0 for the special case of planar, two-dimensional flow. Some very brief results are shown for planar two-dimensional flow. The characteristics of Eqs. (1) and (2) are the right- and left-running Mach lines given by

$$(dy/dx)_\pm = \lambda_\pm = \tan(\theta \pm \alpha), \tag{3}$$

where the subscript + denotes left-running Mach lines and the subscript − denotes right-running Mach lines. The compatibility equation valid on the Mach lines is

$$(u^2 - a^2)\, du_\pm + [2uv - (u^2 - a^2)\, \lambda_\pm]\, dv_\pm - \delta(a^2 v/y)\, dx_\pm = 0. \tag{4}$$

In the numerical work presented later, the algorithm based on Eq. (4) is called scheme 1. By introducing Eq. (3) into Eq. (4), an alternate form of the compatibility equation is obtained:

$$du_\pm + \lambda_\mp dv_\pm - \delta(a^2 v/y)\, dx_\pm = 0. \tag{5}$$

Although Eq. (5) is completely equivalent to Eq. (4), it is much simpler and may result in improved accuracy. The algorithm based on this equation is scheme 3.

A third form of the compatibility equation can be found in terms of the velocity magnitude $V = (u^2 + v^2)^{1/2}$, the flow angle $\theta = \tan^{-1}(v/u)$, and the Mach number M.

$$(\sqrt{M^2 - 1}/V)\, dV_\pm \pm d\theta_\pm - \delta[\sin\theta/yM\cos(\theta \pm \alpha)]\, dx_\pm = 0. \tag{6}$$

The algorithm based on Eq. (6) is scheme 2.

For nondissipative rotational flows, the governing equations are the continuity equation, the two component Euler momentum equations, and the definition of the acoustic speed.

$$\rho u_x + \rho v_y + u\rho_x + v\rho_y + \delta\rho v/y = 0, \tag{7}$$

$$\rho u u_x + \rho v u_y + p_x = 0, \tag{8}$$

$$\rho u v_x + \rho v v_y + p_y = 0, \tag{9}$$

$$up_x + vp_y - a^2 u\rho_x - a^2 v\rho_y = 0. \tag{10}$$

For isentropic, rotational flow, the speed of sound a is a function of pressure and density. Equation (10) could be substituted into Eq. (7) to eliminate derivatives of the density, resulting in a simpler system. However, the above set of equations are in the form of the governing equations for dissipative flows. For example, in nonequilibrium reacting flows a nonhomogeneous term must be added to Eq. (10), and the species continuity equation becomes part of the system of equations. In gas-particle flows, nonhomogeneous terms appear in Eqs. (8)–(10), and the particle drag and energy equations become part of the set. In both cases, the left-hand sides of Eqs. (7)–(10) remain unchanged. Thus, the present set of governing equations was investigated with the hope that some of the general observations would be applicable to dissipative flows. The characteristics of Eqs. (7)–(10) are the Mach lines given by Eq. (3) on which the compatibility equation is

$$(\rho v)\, du_\pm - (\rho u)\, dv_\pm + [\lambda_\pm - u(u\lambda_\pm - v)/a^2]\, dp_\pm - [v(u\lambda_\pm - v)/y]\, dx_\pm = 0 \tag{11}$$

and the streamlines with two compatibility equations:

$$(dy/dx) = v/u = \tan\theta, \tag{12}$$

$$\rho u\, du + \rho v\, dv + dp = 0, \tag{13}$$

$$dp - a^2\, d\rho = 0. \tag{14}$$

The algorithm based on Eqs. (11), (13), and (14) is scheme 4. An alternate form of these equations is found in terms of V, θ, and M.

$$(\sqrt{M^2 - 1}/\rho V^2)\, dp_\pm \mp d\theta_\pm + \delta[v/yMV\cos(\theta \pm \alpha)]\, dx_\pm = 0, \tag{15}$$

$$\rho V\, dV + dp = 0, \tag{16}$$

$$dp - a^2\, d\rho = 0. \tag{17}$$

The algorithm based on Eqs. (15)–(17) is scheme 5.

Thus, a total of five sets of compatibility equations were found. Since irrotational flow is a special case of rotational flow, the rotational flow schemes are valid for irrotational flows also. Hence, a total of five different, but theoretically equivalent, sets of compatibility equations were determined for evaluating irrotational flows. Two distinct sets were determined for evaluating rotational flows. When the two different finite difference schemes are considered (i.e., average coefficients or average properties), ten numerical schemes result for irrotational flow and four for rotational flow. All these schemes were investigated numerically for the same initial conditions in order to study the behavior of the schemes in an attempt to determine the better schemes.

III. Overall Numerical Algorithm

Complete numerical algorithms were developed and programmed for computer evaluation for all of the ten schemes discussed above. All the point schemes were based on extending Mach lines forward from two known points to locate the solution point, and in the case of rotational flow, the streamline was extended backward to intersect the line between the two initial points. Several flows were analyzed in this study. These were: Expanding source flows in conical boundaries; expanding flows in parabolic boundaries; and diffusing sink flows in conical boundaries.

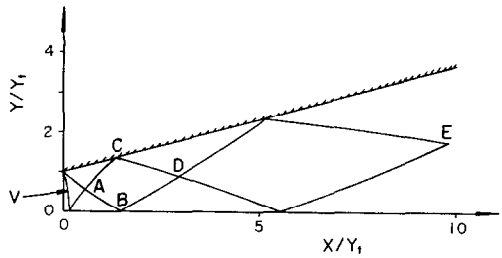

FIG. 3. Overall Mach line pattern in an expanding flow.

Figure 3 illustrates the flow field for the expanding conical source flow. In all the studies, the initial-value line was a circular arc segment of a source flow tangent to the solid wall at the point of intersection. The initial-value line was divided into a number of equally spaced angular increments. The method of characteristics point scheme was applied down right-running Mach lines to the centerline starting first on the initial-value line at the centerline, and then from each higher point on the initial-value line until the wall is reached. At that point, a wall point is determined as the intersection of the left Mach line from the second point on the previous right Mach line, with the wall contour. A right Mach line is then extended

from the new wall point to the centerline, and the process is repeated until the entire flow field has been evaluated. Following this procedure, the entire characteristic network and flow properties at all points of the network are determined.

The singularity in the nonhomogeneous term at the centerline was evaluated as follows. On the centerline,

$$v/y = u(v/u)/y = u \tan \theta/y \simeq u\theta/y. \tag{18}$$

The term is then approximated by evaluating u on the centerline and (θ/y) at the last point on the right-running Mach line above the centerline. This technique is equivalent to requiring that $(\mathrm{d}\theta/dy) =$ constant in the close neighborhood of the centerline. Obviously, other approximations could be employed, and at the outset of this investigation, several other schemes were considered. However, the numerical accuracy obtained with this scheme was comparable with the accuracy of the interior and wall point schemes, so no further studies were made of this approximation.

Figure 3 illustrates selected characteristic curves, namely, those originating on the initial-value line at both the wall and centerline, and their reflections throughout the nozzle. The location of the characteristics are determined from the integration of the characteristic equations, and the flow properties along the characteristics are determined from the integration of the compatibility equations. Accuracy studies should consider both the accuracy of the location of the characteristics, as well as the accuracy of the flow properties on the characteristics. Numerical results were obtained for the location of points A–E shown in Fig. 3, and for the flow properties at these points. These studies were conducted for both irrotational and rotational initial-value lines, various specific heat ratios, a range of initial Mach numbers, both source and sink flows in conical and parabolic contours, and a large range of step sizes, for all ten of the numerical algorithms discussed above. The effect of iterating the corrector to a specified tolerance was investigated. The actual conditions investigated and the results obtained are presented in the following sections.

IV. Accuracy Considerations

When studying the accuracy of a numerical scheme, two different properties are of interest: the absolute error of the scheme, and the order of the accumulated error of the scheme. Two methods exist for determining these quantities. The first method involves calculating the solution of a flow for which an exact solution exists, and then computing the absolute error and order of the scheme directly.

The computed and exact solution can be related as follows:

$$C = E + A_1 h + A_2 h^2 + \cdots + A_n h^n + \cdots, \tag{19}$$

where C is the computed solution, E is the exact solution, h is the step size, and the A_n are proportionality constants which must be determined numerically. For a scheme having nth-order accuracy, the first nonvanishing term in Eq. (19) is $A_n h^n$. In general, nothing can be said about the higher-order terms. However, for sufficiently small step size h, these terms should vanish, and the accumulated error is then proportional to h^n. In the present investigation, these terms were found to vanish by actual numerical computation. However, for flows near a singular point or in regions of extremely large gradients, these terms may not vanish. The order of a scheme can be determined numerically by evaluating the exact error for two step sizes, one half the other, and then determining the ratio of these errors, which is proportional to $h^n/(h/2)^n$, or 2^n. For a second-order scheme, this ratio is 4. This is obviously the best way to evaluate the order of a numerical scheme, but unfortunately, in multidimensional flows, very few exact solutions exist. One exact solution is for expanding source flow or diffusing sink flow in a conical passage. Extensive source flow accuracy studies are presented in this paper. However, source flow is a well-behaved flow with straight streamlines. In order to study flows with curved streamlines, flows in parabolic contours were also investigated. However, no exact solution for such flows is available.

The second method for determining the error and order of error of a numerical scheme requires the numerical evaluation of the exact solution. This can be accomplished with Eq. (19) by computing the solution at a given step size h, then successively halving the step size and recomputing the flow field until enough numerical results are available to evaluate the coefficients A_n which are significant and the exact solution E. From these results, the accuracy and order of the scheme can be determined as discussed above. This method was employed for the flows in parabolic contours. This idea of a deferred approach to the limit (first introduced by Richardson and Gaunt [3]) can sometimes fail, although not in a well-behaved problem such as considered herein.

Thus, by either method, the ratio of the errors for successively halved step sizes can be determined, and this ratio should be approximately 4 for a second-order scheme. The exact step size at which this ratio becomes 4 depends on many factors, but mainly the gradients in the flow. Thus, for a well-behaved flow such as a source flow, the scheme may approach second order at a relatively large step size, whereas for a highly distorted flow such as occurs near a Prandtl–Meyer corner, the scheme may approach second order only for very small step sizes. However, the basic order of the scheme can be determined from smooth flows, and this order would then be expected even in highly distorted flows for some small step

size. Thus, the study of source flow is very useful in determining the order of a scheme.

The accuracy obtainable with the second method discussed above was studied by constructing the characteristic network in a source flow field using a fifth-order Runge–Kutta scheme with a step size of $0.0001y_t$. The Mach lines in any flow are given by the integrals of Eq. (3), which require that $\theta(x, y)$ and $\alpha(x, y)$ be known. In a source flow, these two functions are known from the exact, one-dimensional solution for the source flow. Employing Eq. (3), the functions $\theta(x, y)$ and $\alpha(x, y)$ for source flow, and a fifth-order Runge–Kutta scheme, the locations of points A, B, and C in Fig. 3 were evaluated to a high degree of accuracy. Then the numerical method of characteristics was employed at successively halved step sizes to determine the location of these same points. When these results from the numerical method of characteristics for x and y at points A, B, and C were substituted into Eq. (19) to evaluate numerically the exact location of these points, the locations were predicted by Eq. (19) within $0.00001y_t$ of the position predicted by the fifth-order Runge–Kutta results. These results certainly substantiate the soundness of this second method for evaluating the error of a numerical scheme. Using this scheme, accuracy studies can be performed even in situations where no exact solution exists.

The accuracy studies conducted during this investigation consisted of both comparisons with known exact solutions and comparisons with numerically generated exact solutions. The results are presented in two forms. The first consists of presenting the solution (both location and flow properties) at a given point in the characteristic network as a function of step size. The second consists of presenting the solution for a particular flow property (primarily velocity magnitude V) along the wall or centerline of the flow passage for several step sizes. In all cases, the step size used to correlate the results is the uniform angular step size on the initial-value line. Since the characteristic network follows Mach lines and their reflections from the wall and centerline, the overall grid is self-regulating, and halving the step size on the initial-value line effectively halves the step size throughout the flow field.

A word of caution should be entered here. The ideas of accuracy and order of accuracy presented here, as well as the concept of the modified Euler scheme, are strictly correct for total differential equations. The characteristic and compatibility equations are not strictly speaking total differential equations since the independent direction of differentiation is not the same in all the simultaneous equations. These equations could better be termed total differential relationships which can be solved by the numerical techniques applicable to total differential equations. Thus, it is not obvious that all the concepts discussed above should hold for the numerical method of characteristics. However, during this investigation, it was verified that these concepts do indeed carry over to the present problem.

V. Computer Program Description

The computer program developed during this investigation was written for the *CDC* 6500 computer, which has approximately fourteen significant figures. Thus, round-off error was assumed to be negligible in these studies. A single program was written to accomplish the input, the generation of the initial-value line, and the control of the logic for evaluating the flow field. Twenty completely separate subroutines were employed for evaluation of the properties of each point in the characteristic network: an interior point routine and a boundary point routine based on each of the five sets of compatibility equations for both the average coefficient technique and the average property technique. In this manner, all the numerical results were based on equivalent initial data, and all the flows were obtained in the same overall manner. The twenty computational subroutines were constructed with great care to represent exactly the numerical scheme being employed.

The thermodynamic properties of the fluid were specified in terms of the specific heat ratio γ, nominally 1.2, the gas constant R, nominally 60.0 (ft-lbf)/(lbm-R), the stagnation temperature T_0, nominally 6000 R, and the stagnation pressure P_0, nominally 1000 psia. Variations in these parameters were studied numerically. For cases where T_0 and P_0 are uniform across the initial-value line, the flow will be irrotational. Such flows were analyzed by all the numerical algorithms. Rotational initial-value lines were obtained by specifying arbitrarily a linear variation of T_0 and P_0 across the initial-value line. Such flows were analyzed by the four rotational flow algorithms.

As mentioned earlier, the initial-value line is a source flow whose source angle was nominally chosen as 15 degrees. Points equally spaced in angle along this line comprised the initial-data points. The number of these points was varied through the values of 3, 6, 11, 21, 41, 81, and 161. The bulk of the results were obtained for 3, 6, 11, and 21 initial points.

The wall boundary was specified as either a conical wall or a parabolic wall. In both cases, the wall contour was given as an analytical function $y = \eta(x)$, and the intersection of left-running Mach lines with the wall were determined by solving simultaneously this equation with the equation for a left-running Mach line. All ten boundary subroutines employed the same wall point location scheme.

For source flows, the exact error in flow properties at each point was evaluated by comparing the numerical solution with the exact source flow solution. The exact solution is given by the well-known one-dimensional, isentropic flow functions, which were programmed in terms of the source flow radius at each point in the flow field.

VI. Numerical Studies

Extensive numerical studies were conducted using the schemes discussed in the previous sections. In order to simplify the presentation of the enormous amount of results shown in the following figures, the legend presented in Table I is employed to identify the ten numerical algorithms. In all cases, the open symbols represent schemes based on averaging the entire coefficient of all the differentials, while the closed symbols denote schemes based on evaluating the coefficients at average values of the properties.

TABLE I

Legend for Numerical Schemes

□	Scheme 1, u-v, irrotational, average coefficient
■	Scheme 1, u-v, irrotational, average property
⋈	Scheme 2, V-θ, irrotational, average coefficient
⧓	Scheme 2, V-θ, irrotational average property
○	Scheme 3, u-v, irrotational, average coefficient
●	Scheme 3, u-v, irrotational, average property
◇	Scheme 4, u-v, rotational, average coefficient
◆	Scheme 4, u-v, rotational, average property
△	Scheme 5, V-θ, rotational average coefficient
▲	Scheme 5, V-θ, rotational, average property

The nominal case considered in this study was a 15-degree source flow with $\gamma = 1.2$, $R = 60$ (ft-lbf)/(lbm-R), $T_0 = 6000$ R, and $P_0 = 1000$ psia. Figure 4 presents the exact source flow solution for the velocity along the wall in this flow with the initial Mach number as a parameter. Several features of importance to the numerical investigation can be seen from these results. First, for initial Mach numbers near unity, the initial expansion is highly nonlinear, and a second-order scheme may not demonstrate its second-order accuracy until the step size is very small. In general, when the solution itself is a second-order polynomial, second-order numerical schemes yield very high accuracy. At the higher Mach numbers the solution becomes almost linear, and a second-order numerical scheme should exhibit its second-order behavior even at relatively large step sizes, and the solution should be more accurate than those for the lower initial Mach numbers. All of these characteristics were found in the numerical studies conducted herein.

Once some error has accumulated, the solution is then effectively following a different member of the family of solutions to the differential equations. Thus,

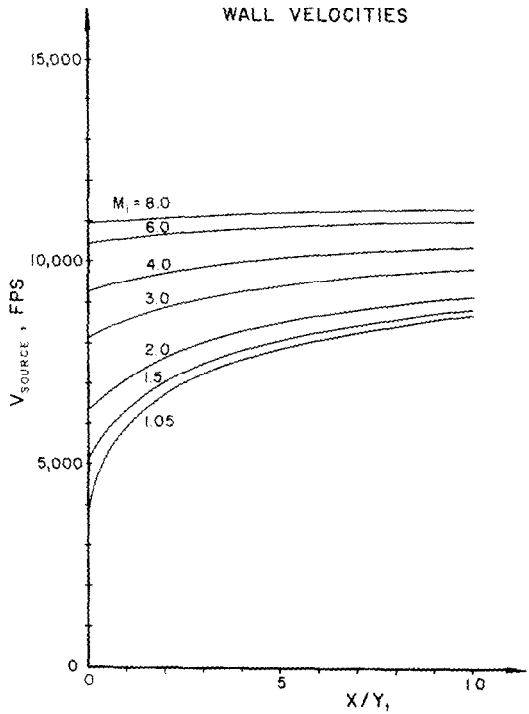

FIG. 4. Exact wall velocities for a 15° source flow, $\gamma = 1.2$, with M_i as a parameter.

when some initially large error is produced for flows near the sonic condition, the numerical solution then tends to follow a different solution curve. However, for expanding flows, all of the solution curves are converging. Thus, large errors created initially should tend to decrease as the solution approaches the higher velocities. For diffusing flows, the opposite is true. The family of solutions diverges, and even small initial errors may result in a large final error. The effect of gradients in stagnation pressure and stagnation temperature should be similar to the effects of gradients in the flow properties. Large stagnation property gradients should require smaller step sizes for comparable accuracy then small or no stagnation property gradients. The combination of large stagnation property gradients and low initial Mach number should result in the most severe limitations on the numerical accuracy. All of these general comments were substantiated by the numerical results obtained during this study.

Basic 15-Degree Source Flow Studies

The nominal case described above was evaluated by all ten numerical algorithms with an initial Mach number of 1.05 and no stagnation property gradients. The

corrector was applied repeatedly until properties converged to a fractional tolerance of 0.00001. The results are presented in terms of values of x, y, V, and θ at points A, B, and C in Fig. 3 as a function of the angular step size $(\Delta\theta/\alpha)$ on the initial-value line. Values of u, v, p, and ρ also could have been presented, but it was found that the trends exhibited by these variables agreed with the trends exhibited by V and θ. Figure 5 presents the results at point A. The exact values at $(\Delta\theta/\alpha) = 0$

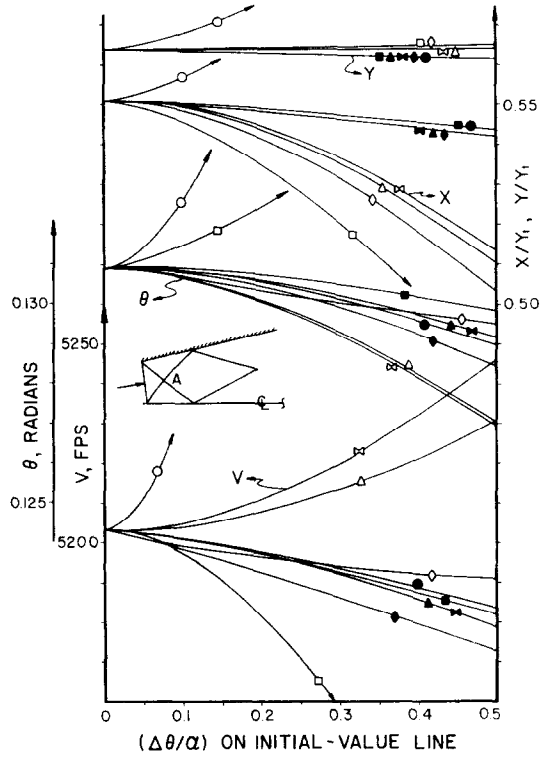

FIG. 5. Error study at point A for a 15° source flow initial-value line with $M_i = 1.05$, 15° half-angle diverging contour, $\gamma = 1.2$.

were obtained from the fifth-order Runge–Kutta results, and substantiated by the numerical evaluation of the exact solution as discussed earlier. The second-order nature of all the schemes is apparent, although some schemes yield better absolute accuracy than others. For instance, schemes 1 and 3 based on averaging coefficients (i.e., □ and ○) both exhibit very poor absolute accuracy. In general, for all five schemes more accurate results were obtained using average property schemes rather than average coefficient schemes. The results shown in Fig. 5 are based entirely on interior point calculations since the effects of neither boundary

are felt at this point. One of the most surprising results of the entire numerical investigation was the change in the absolute accuracy of scheme 3 from very poor accuracy based on averaging coefficients to one of the most accurate when based on averaging properties. This result was found consistently in all the studies at all step sizes, initial Mach numbers, source angles, and specific heat ratios. An attempt to explain this behavior theoretically was not successful. Unexpected and unexplainable results such as this vividly demonstrate the value and necessity of carefully executed accuracy studies.

In Fig. 6, the numerical results for the nominal case are presented at point B. The solution at this point is influenced by both the interior point scheme and the centerline scheme, but not by the solid boundary scheme. Since θ and y are zero, only V and x values are presented. All ten schemes exhibit second-order accuracy, with scheme 3 exhibiting the same peculiar behavior. The x location appears to

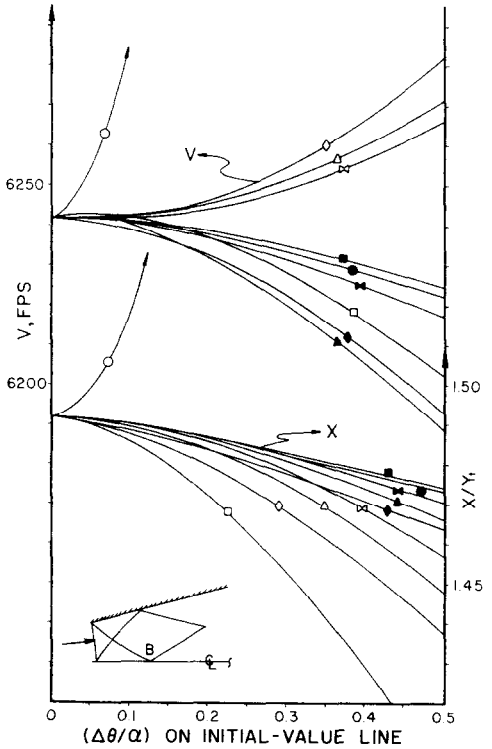

FIG. 6. Error study at point B for a 15° source flow initial-value line with $M_i = 1.05$, 15° half-angle diverging contour, $\gamma = 1.2$.

The properties at point C are influenced by the interior and wall point schemes, but not by the centerline point scheme. Since $y = \eta(x)$ and $\theta = 15$ degrees, Fig. 7 presents only V and x values. The average property schemes are all superior to all the average coefficient schemes. The second-order accuracy of all the schemes is evident.

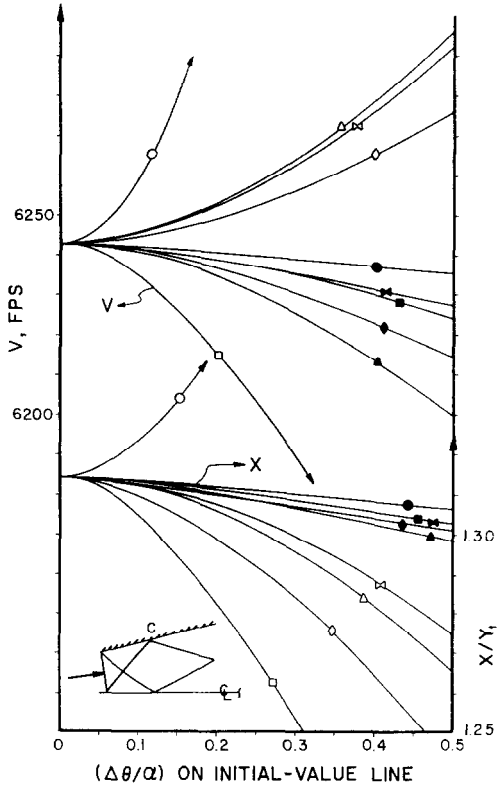

FIG 7. Error study at point C for a 15° source flow initial-value line with $M_i = 1.05$, 15° half-angle diverging contour, $\gamma = 1.2$.

Similar results were obtained at points D and E. The main difference was in increased scatter of the results observed as the point of observation moved down the nozzle, which is indicative of the increasing interplay of the errors as the solution proceeds.

Based on the results presented in Figs. 5–7, it appears that schemes based on average properties are somewhat superior to schemes based on average coefficients. Scheme 3, which has the least complex compatibility equation, was found to be

highly inaccurate for the average coefficient scheme and highly accurate for the average property scheme. Most of the schemes exhibited reasonable absolute accuracy even for step sizes of $(\Delta\theta/\alpha) = 0.5$, in which only three points were specified on the initial-value line. All the schemes exhibited second-order accuracy at all points investigated, although the scatter increased as the solution progressed down the flow field. Since this flow was irrotational, both the rotational and irrotational schemes were employed in the comparison, and it appears that the rotational flow schemes have accuracy comparable to the irrotational flow schemes in spite of the potentially larger error due to locating the streamline, interpolating for its initial properties, and integrating two additional compatibility equations. These results suggest the use of rotational flow schemes even for irrotational flows; thus a single program would be capable of handling both types of flows.

Variations of the Basic Studies

The investigations presented in the basic studies were repeated for several variations around the nominal case. These were: a parabolic wall, a specific heat ratio of 1.4, an initial Mach number of 1.5, and gradients in the stagnation properties. The results of these studies enforced the conclusions drawn above based on the basic studies.

Figure 8 presents the solution at point D for a parabolic wall having an initial angle of 15 degrees to match the source flow initial-value line, and an exit angle of 10 degrees. This flow is obviously not a severely distorted flow, but it does involve some streamline curvature. The results illustrate the second-order accuracy of the scheme, and suggest that the rotational flow techniques are slightly more accurate. Again, the average property schemes are generally superior to the average coefficient schemes. Similar results were obtained for parabolic walls with exit angles of 5 degrees.

Results analogous to Fig. 5, for $\gamma = 1.4$ instead of 1.2, were obtained. Again, the schemes were second-order, the accuracy was comparable to that obtained for $\gamma = 1.2$, and the rotational flow schemes appeared to be the most accurate. The average property schemes were again generally superior.

All of the results presented so far were for an initial-value line Mach number of 1.05, which resulted in large property gradients in the neighborhood of the initial-value line. Figure 9 presents results analogous to Fig. 5, for $M_i = 1.50$ instead of 1.05. Due to the smaller gradients, more accurate results are expected, and this is the case as can be seen by comparing the two figures. All of the trends are the same, except that the scatter with increasing step size has been decreased. Again, the average property schemes appear to be the most accurate. Similar studies were conducted for initial Mach numbers of 1.1, 1.2, 2, 3, 4, 6, and 8. In all cases, the general trends were the same.

Studies were also conducted for rotational initial-value lines. These lines were

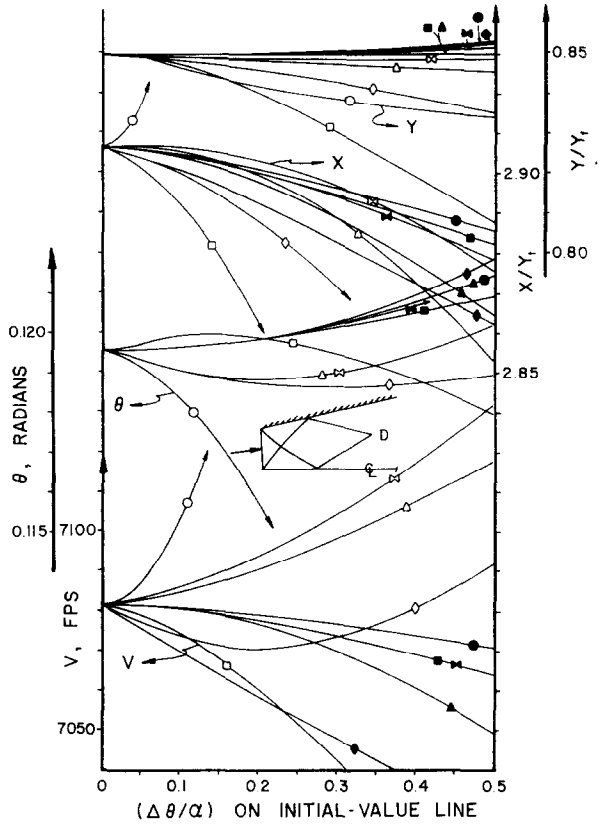

FIG. 8. Error study at point D for a 15° source flow initial-value line with $M_i = 1.05$, parabolic contour from 15° entrance to 10° exit, $\gamma = 1.2$.

obtained by specifying the Mach number and stagnation properties at the wall on the initial-value line, a linear stagnation property gradient across the flow, and a uniform static pressure across the same spherical surface employed as the initial-value line in the previous studies. A stagnation pressure increase of 100 psi was specified, and stagnation temperature increases of both 500 R and 1000 R were investigated. Figure 10 presents the solution at point A for an initial Mach number of 1.05 and a stagnation temperature gradient of 1000 R. Since the flow is now rotational, results are presented only for schemes 4 and 5. This combination of low initial Mach number and large stagnation property gradients should result in a severe test of the schemes. As seen in the figure, all the schemes are second-order for sufficiently small step size. The scatter in the results as the step size increases is large, as expected. Overall, the average property schemes appear more

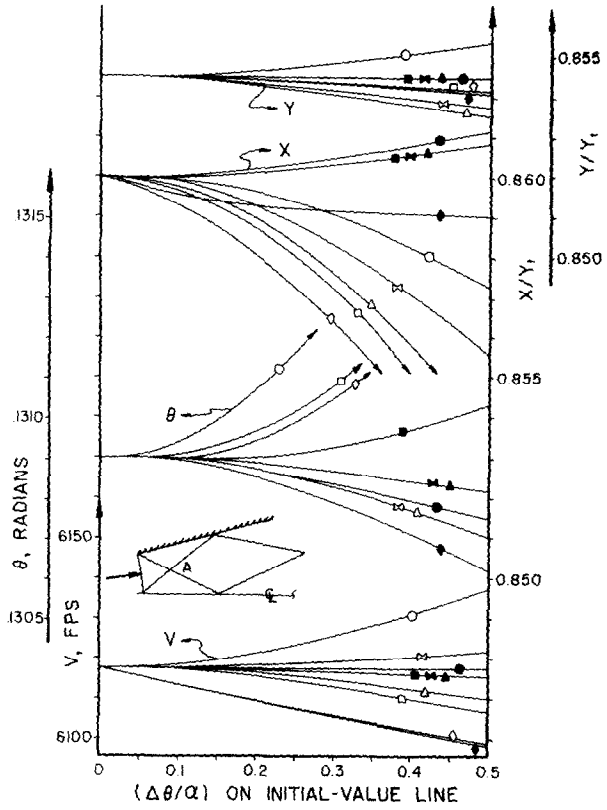

FIG. 9. Error study at point A for a 15° source flow initial-value line with $M_i = 1.50$, 15° half-angle diverging contour, $\gamma = 1.2$.

accurate. Similar results were obtained for the same stagnation property gradients but an initial Mach number of 2.0. The results were second-order, and the absolute accuracy was extremely good. Studies with a stagnation temperature change of only 500 R and the same two initial Mach numbers produced accuracies in between the results of the two previous cases and the results with constant stagnation properties. These results suggest that gradients in stagnation properties must be given serious consideration when selecting the step size, especially in flows near the sonic condition. The combination of high flow gradients near the sonic condition and large stagnation property gradients combine to decrease further both the absolute accuracy and order of accuracy of the scheme.

Wall and Centerline Velocity Studies

From the results already presented, it appears that scheme 5 is representative of the best accuracy which can be obtained by the axisymmetric method of char-

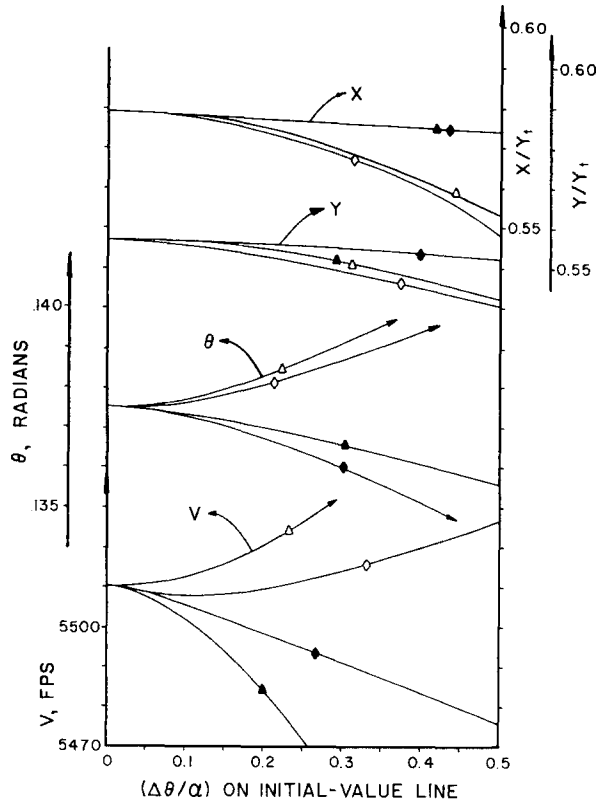

FIG. 10. Error study at point A for a rotational initial-value line with $\Delta P = 100$ psi and $\Delta T = 1000\,^{\circ}\mathrm{R}$, $M_i = 1.5$, 15° half-angle diverging contour with $\gamma = 1.2$.

acteristics. In this section, results for the wall and centerline velocities are presented for scheme 5 to illustrate further the properties of the numerical algorithm. All of these studies employed the nominal case data. Figure 11 presents the error in velocity along the wall as a function of step size on the initial-value line for both the average coefficient and the average property techniques. From these results, the second-order behavior of the scheme is clearly evident. The bumps in the average coefficient curves occur where the second reflection of the Mach line of the initial-value line and the centerline intersects the wall. The sudden jumps in the average property curves occur at the first intersection with the same Mach line. A point of great interest shows clearly on these curves. This is the initial large error incurred on the very first point on the wall. This initial error itself is also clearly second-order. The cause of this large initial error is the steep flow gradients on the initial-value line, which in this case has a Mach number of 1.05.

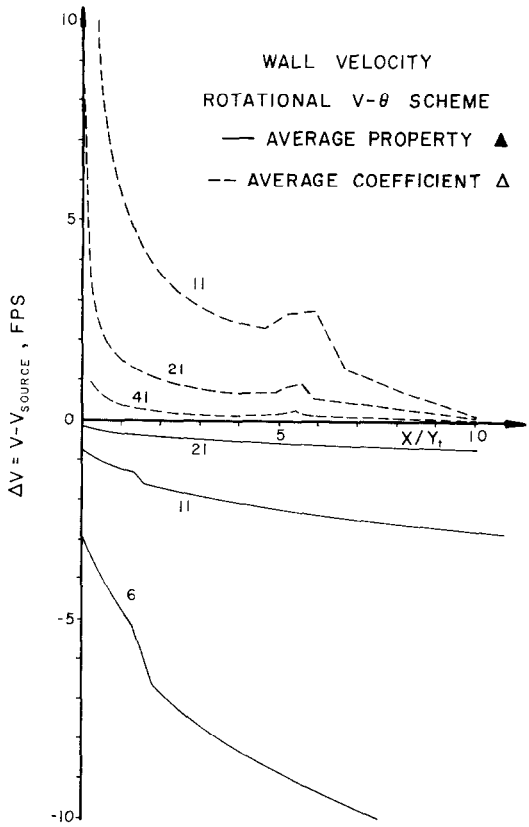

FIG. 11. Error study along the wall for a 15° source flow initial-value line with $M_i = 1.05$, 15° half-angle diverging contour, $\gamma = 1.2$, scheme 5, with 6, 11, 21 and 41 points on the initial-value line.

This large initial error was present in all studies when the initial value Mach number was near unity. This occurs because the coefficients in the differential equations may change magnitude by as much as a factor of 2 within a point evaluation when the Mach number is near unity. For example, the coefficient $(u^2 - a^2)$ in scheme 1 roughly doubles when the Mach number changes from 1.05 to 1.10. Once the initial steps have been taken, the region of high gradients has been completed and the errors diminish greatly in magnitude. The fact that the errors tend toward zero is a fortuitous combination of the basic characteristics of the numerical algorithm and the converging nature of the velocity field. These results suggest that very small step sizes are required when the flow is near the sonic condition. Although not investigated here, it seems feasible that some large

number of initial-value line points, such as 41, could be used to advance the initial-value line one, two, or three steps out into the flow field, where the number of points could then be reduced considerably for the remainder of the solution.

Figure 12 presents the centerline velocity error for the same conditions of Fig. 11. These results substantiate the conclusions drawn from Fig. 11. The discontinuities occur where the first Mach line from the wall intersects the centerline. From both these figures, it is evident that the average property scheme results in an error of approximately only one-half the error of the average coefficient scheme. This characteristic was observed in most of the results obtained during this investigation. As a result, the average property scheme is recommended over the average coefficient scheme.

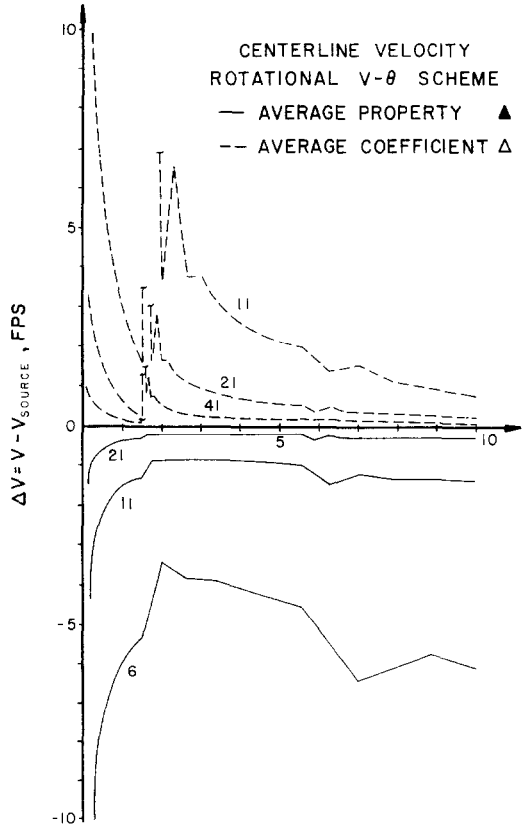

FIG. 12. Error study along the centerline for a 15° source flow initial-value line with M_i = 1.05 15° half-angle diverging contour, γ = 1.2, scheme 5, with 6, 11, 21 and 41 points on the initial-value line.

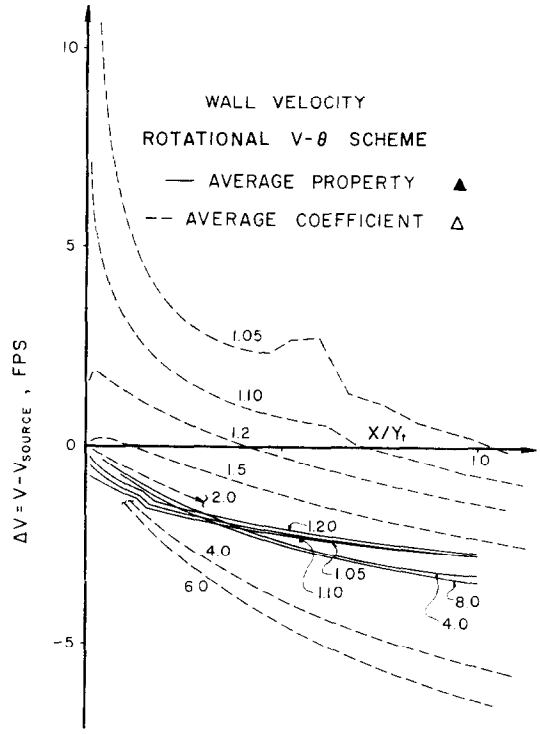

FIG. 13. Error study along the wall for a 15° source flow initial-value line with 11 points 15° half-angle diverging contour, $\gamma = 1.2$, with $M_i = 1.05, 1.1, 1.2, 1.5, 2, 4, 6$, and 8, scheme 5.

Figure 13 presents results for the same nominal conditions as in Figs. 11 and 12, with the initial-value line Mach number as a parameter. The effect of the large gradients near the sonic condition is clearly evident. Both schemes, the average property and average coefficient techniques, are basically under-predicting schemes once the initial error due to the large gradients has been made. As the initial Mach number is increased, the initial error approaches zero, and the error then grows in a bounded monotonic fashion, as expected. These results clearly favor the average property scheme and the use of a large number of initial-value line points for near sonic flows. Eleven initial-value line points were used.

Comparison of Prodicting, Correcting, and Iterating

Several possibilities exist in the development of the overall algorithm. All the schemes presented in this study are based on an Euler predictor and a modified Euler corrector, with or without iteration. In this section, a comparison is made of several of these possibilities.

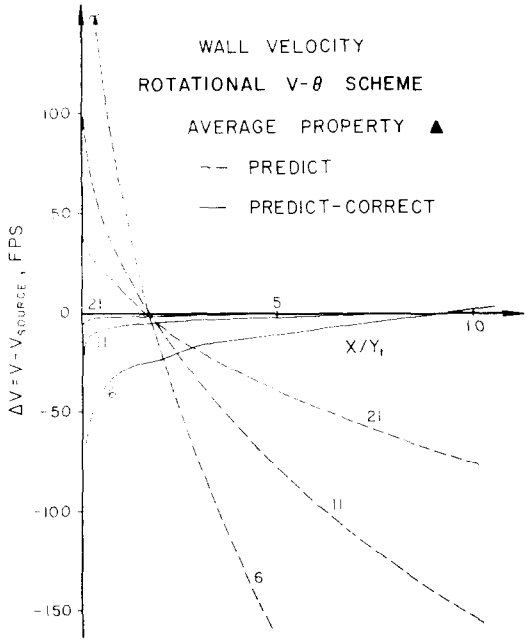

FIG. 14. Error study along the wall for a 15° source flow initial-value line with $M_i = 1.05$, 15° half-angle diverging contour, $\gamma = 1.2$, scheme 5, with 6, 11 and 21 points on the initial-value line, illustrating predict only and predict–correct once results.

Figure 14 presents the error in wall velocity for the nominal conditions of this investigation as calculated by scheme 5 using the average property technique. The dashed curves were obtained using only the Euler predictor, which theoretically should be first order, as it clearly is. The solid curves were obtained with one application of the modified Euler corrector, which is theoretically and numerically second order. A tremendous improvement in absolute accuracy is also obtained with the corrector. Similar results were obtained with the other four schemes with both the average property and average coefficient techniques. These results clearly demonstrate the desirability of the higher-order scheme.

However, it is not clear whether or not the repeated application of the corrector is worthwhile. This question is studied in Fig. 15, where the same conditions as in Fig. 14 were investigated by scheme 5 with both the average property and average coefficient techniques. Results are presented for one, two, and three applications of the modified Euler corrector. The basic character of the average coefficient scheme is unchanged by repeated applications of the corrector. The basic character of the average property scheme appears to change from an over-predicting to an under-predicting scheme. However, in both cases, no advantage

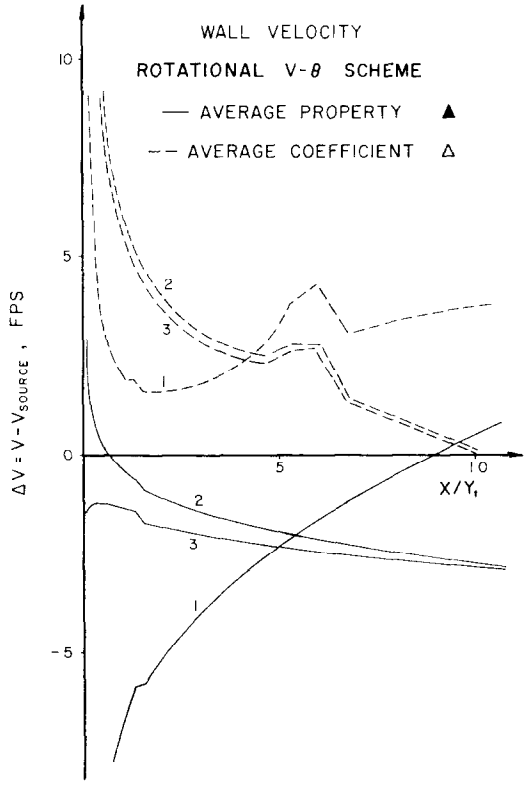

FIG. 15. Error study along the wall for a 15° source flow initial-value line with $M_i = 1.05$, 15° half-angle diverging contour, $\gamma = 1.2$, scheme 5, with 11 points on the initial-value line, illustrating the effects of the number of applications of the corrector.

seems to occur due to the repeated application of the corrector, except for the decrease in initial error observed for the average property scheme. This is a general conclusion substantiated by all the studies conducted during this investigation.

Figure 16 presents results for the same conditions as studied in Fig. 15, with the corrector applied repetitively until the solution converged to within a specified fractional tolerance. These results clearly demonstrate that converging to a fractional tolerance smaller than 0.001 is of no benefit. In fact, the results for a tolerance of 10^{-8} in some cases required as much as twice the computer time as the 10^{-3} results with no change in the solution. A fractional tolerance of 0.01 generally yields a predict–correct once solution, particularly for the average coefficient case. However, for the average property case, the large (relatively speaking) initial error shown on Fig. 15 has been eliminated, and the bulk of the 10^{-2} and correct-once results are comparable. These results suggest the use of a coarse

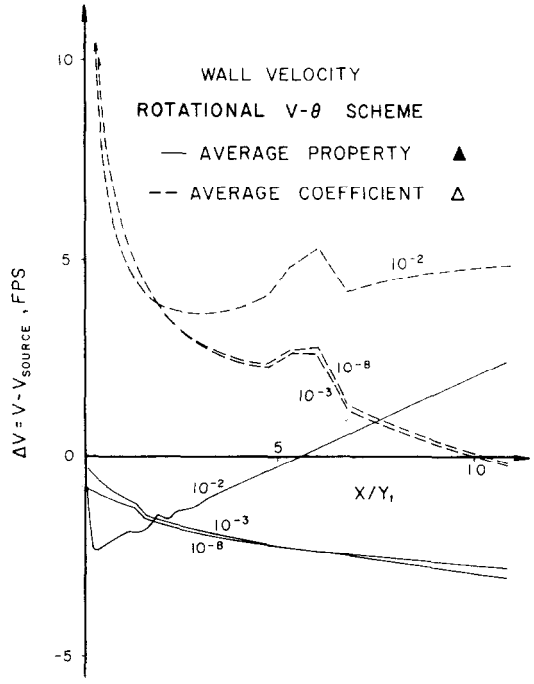

FIG. 16. Error study along the wall for a 15° source flow initial-value line with $M_i = 1.05$, 15° half-angle diverging contour, $\gamma = 1.2$, scheme 5, with 11 points on the initial-value line, illustrating the effect of a fractional convergence tolerance.

convergence tolerance such as 0.01 to 0.005, which generally results in a predict–correct once scheme except in regions of large gradients where several applications of the corrector may be required. This conclusion was reached for all the numerical schemes studies during this investigation. Thus, iteration to a tight fractional tolerance does not appear to be warranted in any case.

Comparison of Grid Schemes

In Fig. 2, three different grid schemes were illustrated for the rotational flow method of characteristics. Scheme III was employed throughout all the investigations presented heretofore. An investigation was made of these three grid schemes using method of characteristics scheme 5 based on average properties. Additionally, left-running Mach lines were forced to intersect the wall at equally spaced points, from which right-running Mach lines were reflected into the flow field. The centerline intersections were performed as before, by simply reflecting the incident right-running Mach waves back into the flow field. Studies were conducted for the

nominal conditions with 11, 21, and 41 initial-value line points. The results are presented in Fig. 17. All three schemes are clearly second order, and the absolute accuracy of all three is almost equal. The large initial errors due to the large gradients near the sonic point are evident. Based on studies such as this, it was concluded that the three grid schemes yield comparable results, and the choice

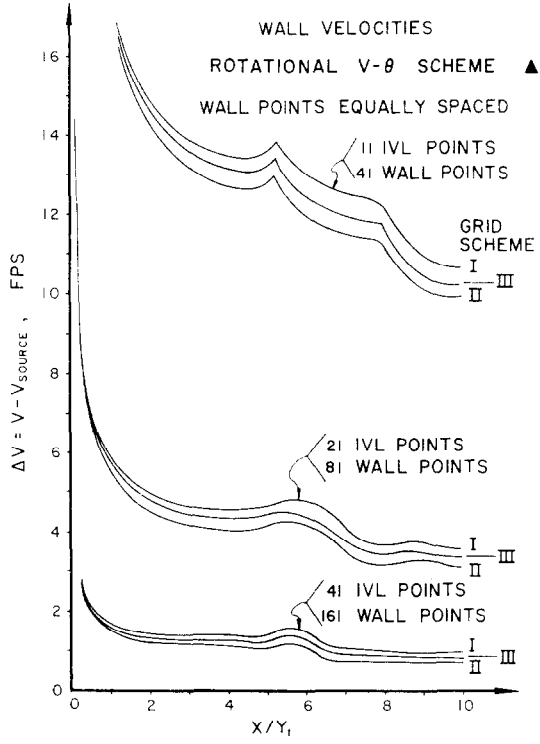

FIG. 17. Error study along the wall for a 15° source flow initial-value line with $M_i = 1.05$, 15° half-angle diverging contour, $\gamma = 1.2$, Scheme 5, with 11, 21, and 41 initial-value line points, illustrating the differences between the three characteristic net grid schemes shown in Fig. 2.

between them must be based on other considerations. Scheme III was employed during the present investigations for two reasons: first, the streamline length is smaller than for either of the other two methods, and second, some simplifications in programming logic are possible with this scheme. It should be stressed that these results apply only to nondissipative flows. For dissipative flows, such as gas-particle flows and nonequilibrium, reacting flows, the characteristic grid scheme should be based on the streamline and either of the two Mach lines, instead of the two Mach lines as chosen in the present investigations.

Results for Diffusing Flows

All of the results presented so far have been for expanding flows, with their favorable converging solution character. Diffusing flows have the opposite character, the solution curves being closely spaced at the high Mach numbers and diverging as the Mach number decreases. This can be seen in Fig. 4 for the wall velocity in a 15 degree sink flow by realizing that the flow progresses from high to low velocities in a diffusing flow. As demonstrated in Fig. 13, the initial errors in flows with large initial Mach numbers are small, and they grow in a bounded manner. This same small initial error should occur in diffusing flows starting at high initial Mach numbers, but the error should grow rapidly as the flow approaches the lower Mach numbers. In fact, near the sonic condition, the error may grow without bound. Figure 18 presents the wall pressure for a diffusing 15 degree sink flow with an initial Mach number of 3.0. These results were obtained

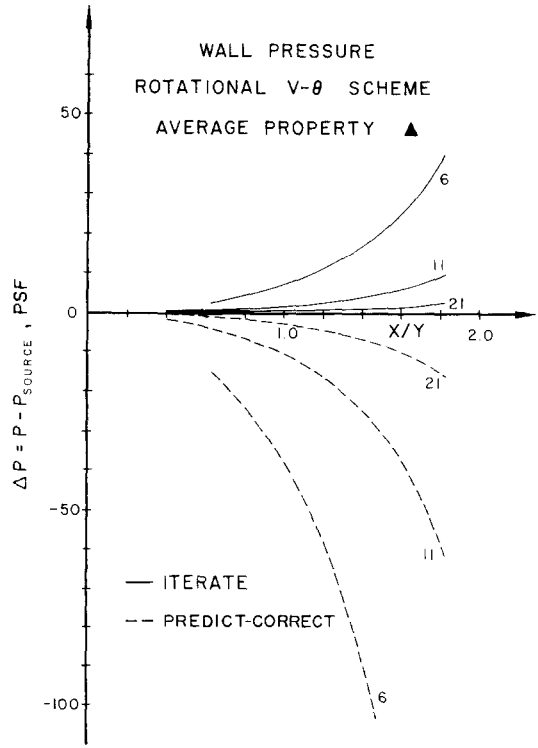

FIG. 18. Error study along the wall for a 15° sink flow initial-value line with a Mach number $M_i = 3.0$, 15° half-angle converging contour, $\gamma = 1.2$, scheme 5, with 6, 11, and 21 points on the initial-value line.

with scheme 5 using the average property technique, both for the predict–correct scheme and for iteration to a fractional tolerance of 0.000001. From these results, it is seen that the scheme is clearly second order. In addition, the initial errors are extremely small. As expected, the errors grow rapidly as the flow decelerates, and the error growth rate appears unbounded. In this case of diffusing flow, the use of iteration appears worthwhile. Similar results were obtained for the other numerical schemes. These results suggest that a coarse grid may be employed initially in high Mach number diffusing flows, and that the grid spacing should be decreased as the Mach number decreases, approaching the range of 21 to 41 points across the flow when the sonic condition is approached.

Studies such as those presented in Figs. 5–16 for accelerating flows were conducted for diffusing flows. In general, all of the conclusions reached for the accelerating flows were valid for the diffusing flows, except for the use of iteration, which appears worthwhile for diffusing flows. The only major difference in the results is the unbounded error growth discussed in conjunction with Fig. 18.

Some Two-Dimensional Results

Several of the studies described above were conducted for planar, two-dimensional flow. In general, the conclusions reached for axisymmetric flows are valid for two-dimensional flow. The major difference is in the magnitude of the absolute

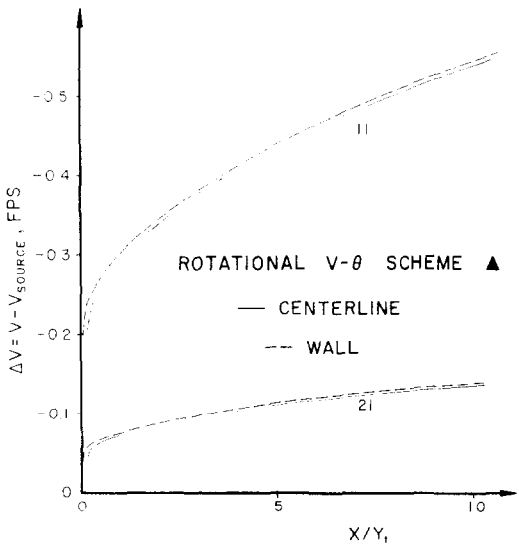

FIG. 19. Error study along the wall and centerline for a 15° source flow initial-value line with $M_i = 1.05$, 15° half-angle diverging contour, $\gamma = 1.2$, scheme 5, with 11 and 21 points on the initial-value line, for a planar, two-dimensional flow field.

accuracy, which was much better for the two-dimensional flows. This was expected since the flow gradients are much smaller in two-dimensional flows. As an example, Fig. 19 presents the wall and centerline velocity distributions for the nominal conditions discussed earlier, for scheme 5 with average coefficients. As illustrated, the initial error is small, and the error grows in a bounded manner. The centerline and wall solutions have comparable accuracies since the nonhomogeneous term of axisymmetric flow is not present. The solution is clearly second order. These results can be compared with the equivalent axisymmetric case, presented in Figs. 11 and 12. In addition to the different trends discussed above, it is seen that the level of error is ten times smaller than in the axisymmetric case. Thus, for comparable accuracy, much larger step sizes may be taken in planar, two-dimensional flows as compared with axisymmetric flows.

CONCLUSIONS

The results of these studies, although strictly valid only for the conditions actually investigated, suggest some general guidelines for the application of the numerical method of characteristics to axisymmetric, supersonic flows. For rotational flows, a grid scheme based on following Mach lines and extending the streamline back to intersect the line between the two initial points is satisfactory. For irrotational flows, the results obtained with rotational flow schemes were of comparable accuracy, suggesting the exclusive use of rotational flow schemes in order to obtain a single scheme capable of handling both irrotational and rotational flows. In many cases, the results based on the average property schemes were more accurate than those based on the average coefficient schemes. Thus, the use of the average property scheme is recommended. The results of the studies of predict, predict–correct, and iterate, clearly suggest the use of a predict–correct once scheme with a coarse convergence tolerance overriding in regions of high gradients. In regions of large flow gradients or stagnation property gradients, a large number of grid points is required. For expanding flows, the number of points can be decreased as the solution progresses, but for diffusing flows, the opposite trend must be enforced. Some limited results for two-dimensional flow demonstrated the superior accuracy attainable for such flows. Overall, these studies present a favorable picture of the accuracy attainable by the numerical method of characteristics. It is hoped that these studies will encourage other similar studies, and thus greatly expand the understanding of the behavior of the numerical method of characteristics.

ACKNOWLEDGMENT

At the beginning of this investigation, Prof. Robert Lynch of Purdue University was of great assistance in planning the approach taken. During the course of the studies, numerous discussions with Dr. M. Cline of Purdue University were very helpful in the interpretation of the results. The generous assistance of both is appreciated and acknowledged.

REFERENCES

1. R. SEDNEY, A survey of the method of characteristics for nonequilibrium, internal flows, Paper No. 69-6, AIAA Seventh Aerospace Sciences Meeting, New York, Jan., 1969.
2. J. H. GIESE, Approximate methods for computing flow fields, *Comm. Pure Appl. Math.* **7** (1954), 65–67.
3. L. F. RICHARDSON AND J. A. GAUNT, The deferred approach to the limit, *Phil. Trans. Royal Soc. London Ser. A* **229** (1927), 299–361.